American Journal of Ophthalmology Case Reports 1 (2016) 16–22

Contents lists available at ScienceDirect

American Journal of Ophthalmology Case Reports

journal homepage: http://www.ajocasereports.com/

Case report

Parafoveal cone abnormalities and recovery on adaptive optics in posterior uveitis

Kristin Biggee [c], Michael J. Gale [a], Travis B. Smith [a], Eric B. Suhler [a, b, 1], Mark E. Pennesi [a], Phoebe Lin [a, *]

[a] Casey Eye Institute, Oregon Health & Science University, Portland, OR, USA
[b] Department of Ophthalmology, Veteran's Affairs Medical Center, Portland, OR, USA
[c] Kaiser Medical Group Salmon Creek, 14406 NE 20th Ave, Vancouver, WA 98686, USA

ARTICLE INFO

Article history:
Received 15 December 2015
Received in revised form
18 February 2016
Accepted 8 March 2016
Available online 11 March 2016

Keywords:
Adaptive optics
Posterior uveitis
Photoreceptors
Optical coherence tomography
Autofluorescence

ABSTRACT

Purpose: To determine if adaptive optics (AO) flood illumination imaging can detect subclinical changes in 4 cases of posterior uveitis affecting the outer retina.
Observations: In all 4 cases, the affected eye showed altered areas in the photoreceptor mosaic on AO that corresponded to changes on other imaging modalities. Abnormalities not apparent on other imaging modalities were also noted. In one case of multifocal choroiditis with acute outer retinal atrophy, AO revealed decreased visualization of photoreceptors in the unaffected eye that was not noted on spectral domain-optical coherence tomography. In the patient with multiple evanescent white dot syndrome, focal photoreceptor abnormalities were more apparent on AO compared to other imaging modalities, and these areas normalized on AO during follow-up. Five weeks after initiation of high dose prednisone and azathioprine in a patient with serpiginous choroidopathy, AO images showed recovery in apparent parafoveal cone density.
Conclusions and importance: AO detects subclinical changes in the photoreceptor layer in posterior uveitis that can recover over time. AO may be useful in following outer retinal inflammatory conditions.

1. Introduction

Posterior uveitis (PU) encompasses a heterogeneous group of disorders with a predominant site of intraocular inflammation located in the retina or choroid. Spectral domain optical coherence tomography (SD-OCT) and fundus autofluorescence (FAF) have allowed non-invasive *in vivo* imaging that is able to distinguish and localize abnormalities in the outer retina and RPE in many cases of posterior uveitis. Studies showing the utility of multi-modal imaging in posterior uveitis have been growing in number [1–10].

Adaptive optics (AO) has been used to study a variety of retinal conditions including the normal cone mosaic, acquired and inherited retinal disorders, and color deficiencies [11–17]. There are few case reports and one larger series of AO use in uveitis [2,18–22]. With the exception of the larger case series and one case report utilizing AO-OCT, most case reports utilize custom-built AO-scanning laser ophthalmoscopy (SLO) systems and showed photoreceptor abnormalities in the diseased eye, but to our knowledge seldomly demonstrated improvements in these changes after treatment or time. In our study, we demonstrate the ability of a commercially available AO flood-illuminated camera to document alterations in the parafoveal cones in posterior uveitis, including subclinical changes not seen on other commonly used imaging modalities, and reversibility of these AO abnormalities in some cases.

2. Methods

This research was approved by the Institutional Review Board of the Oregon Health & Science University and adhered to the tenets of the Declaration of Helsinki. All subjects signed an informed consent after the nature and possible consequences of the study

* Corresponding author. Casey Eye Institute, Oregon Health and Sciences University, 3375 SW Terwilliger Blvd, Portland, OR 97239, USA.
E-mail address: linp@ohsu.edu (P. Lin).
[1] Dr. Suhler is a member of the editorial board of the *American Journal of Ophthalmology Case Reports* but was not involved in the review of this manuscript or making of the final decision.

http://dx.doi.org/10.1016/j.ajoc.2016.03.001

were explained. Permission was obtained to publish personal information such as age, gender, and ethnicity.

Both eyes of 4 sequentially recruited subjects with posterior uveitis were imaged using the Rtx1 AO camera (Imagine Eyes, Orsay, France). Exclusion criteria included patients with opacification of the ocular media, subjects that had uncontrolled nystagmus, trembling, or movements of the eyes and/or head that prevented target fixation, or incapacity to maintain a stable position while seated. Both eyes were dilated with 1% phenylephrine and 2.5% mydriacyl prior to each imaging session. The same technician conducted all imaging sessions in the study.

The scanning protocol consisted of a series of 25, 4° × 4° images with 40 raw images at each point, acquired with 50% overlap between adjacent images, then automatically registered and combined to reduce noise and enhance image quality using vendor-provided software (ck_v0_1b, Imagine Eyes, Orsay, France) to cover a 12° × 12° field of central macula. Automated cone identification was performed using a custom algorithm developed in MATLAB (Mathworks, Natick, MA, USA), and Voronoi cone density maps produced as previously described [23]. Because Rtx1 is unable to detect individual cones at the fovea where the inter-cone spacing is smaller than the spatial resolution, cone density maps in this study have a gray oval to mask these areas [23]. Because inflammation can potentially change the reflective properties of a cone below the threshold of detection on the cone density map, we used the term “decreased apparent cone density” to illustrate the fact that rather than disappearing, the cones may have diminished wave-guiding ability. AO images were compared to corresponding areas from other imaging modalities including fundus images (Optos 200TX, Scotland, UK), FAF (Optos 200TX), infrared photography (IR) (Spectralis, Heidelberg, Germany), fluorescein angiography (FA) (Optos 200TX), and SD-OCT (Spectralis), when obtained for clinical purposes.

2.1. Findings

2.1.1. Case report 1

A 60 year-old Caucasian woman presented with an acutely enlarging scotoma in the left eye. Her corrected visual acuity was 20/20 in both eyes. Examination revealed outer retinal lesions emanating in a serpentine fashion from the optic nerve OS (Fig. 1C). There were no anterior chamber cells, few anterior vitreous cells, and characteristic fluorescein angiographic findings with early hypofluorescence and late hyperfluorescence most prominent at the edges of lesions (Fig. 1D,E). After tests for infectious etiologies including syphilis and tuberculosis came back negative, the patient was diagnosed with serpiginous choroidopathy. AO imaging at the initial visit of the symptomatic left eye illustrated a significant area of decreased cone visualization in the nasal macula corresponding to locations of ellipsoid zone (EZ) or inner segment-outer segment junction (IS/OS) disruption seen on SD-OCT and hyper-autofluorescence on FAF (Figs. 1F, H and 2B). The transition from normal to abnormal cone reflectivity on AO is shown as a magnified AO inset in Fig. 1G, and corresponds to the transition of abnormal to normal EZ and ELM reflectivity on SD-OCT in Fig. 1H. Additionally, the AO cone density map revealed an overall apparent depression in the parafoveal area compared to normal subjects (example of normal subject shown in Fig. 1A, B), in both eyes that was not represented by any evident SD-OCT or FAF abnormalities (Fig. 2). Five weeks after initiating prednisone and azathioprine, the patient symptomatically improved and AO images in the left eye showed persistent areas of decreased cone visualization in the nasal macula that corresponded to the EZ abnormalities on SD-OCT and was represented by initial hyperautofluorescence on FAF (Fig. 2B,J,L). Persistent AO abnormalities appeared to correspond to areas of

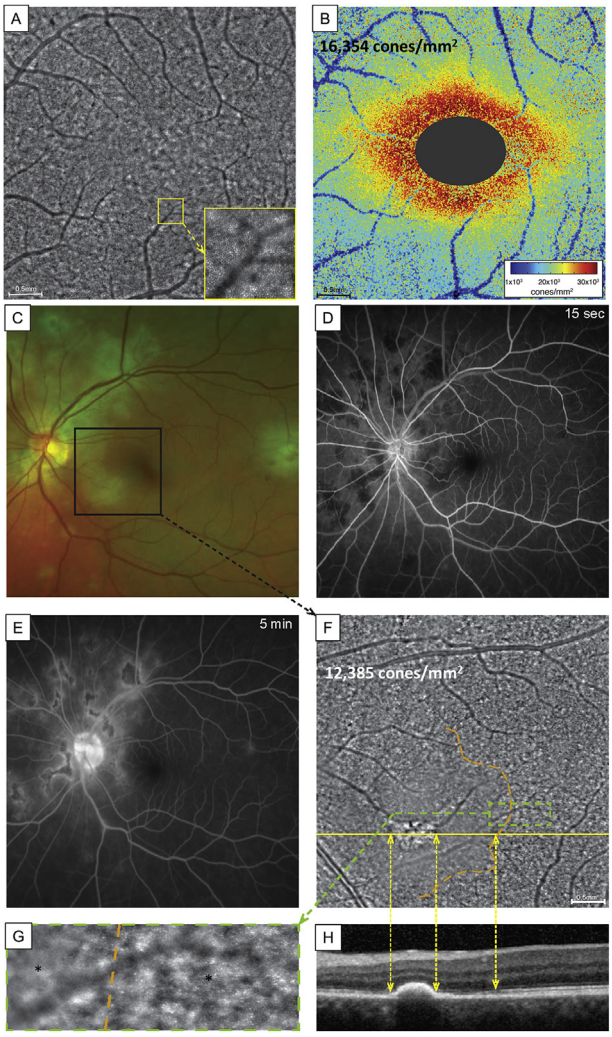

Fig. 1. Reduced cone visualization in adaptive optics (AO) images in serpiginous choroidopathy (Case 1) compared to normal subject. (A) AO composite montage and (B) Voronoi cone density map from a *healthy control subject*. (C) Fundus image and (D,E) fluorescein angiography of Case 1 subject's symptomatic left eye. (F,G) AO composite montage demonstrating focal area of AO hyperreflectivity corresponding to pigment epithelial elevation on spectral domain-optical coherence tomography (SD-OCT) (H) and adjacent area of decreased cone visualization outlined by the orange dotted line. (G) Magnified AO montage showing transition zone from area of abnormal cone mosaic (left side of panel) to area of normal cone mosaic (right side of panel) with asterisks denoting location of 200 μm × 200 μm box where cone densities were quantified at 4477 cones/mm^2 on the left, and 20,825 cones/mm^2 on the right; (H) corresponding SD-OCT changes in the ellipsoid zone and external limiting membrane.

external limiting membrane (ELM) disruption on SD-OCT (dotted arrow, Fig. 2F,J). As shown in the figure, cones in the nasal region remained at low density (from 4451 cones/mm^2 to 5170 cones/mm^2) before and after treatment. The parafoveal apparent cone density, however, showed a recovery in both eyes, suggesting that AO may identify abnormalities in the photoreceptors not seen on SD-OCT, which can recover with treatment (Fig. 2E–J). For instance, despite the minimal improvement in nasal regional cone density, parafoveal cone densities showed a dramatic improvement from 15,847 cones/mm^2 to 21, 979 cones/mm^2 (Fig. 2F,J), a difference of over 6000 cones/mm^2. Global cone densities over the entire 12° x 12° area of retina imaged are listed in the apparent cone density maps or montage in Figs. 1 and 2 and reveal increases in total apparent cone densities of 896 cones/mm^2 OD and 344 cones/mm^2 OS after treatment. Note that global cone densities in the nasal offset montage of the left eye shown in Fig. 1F (image taken at

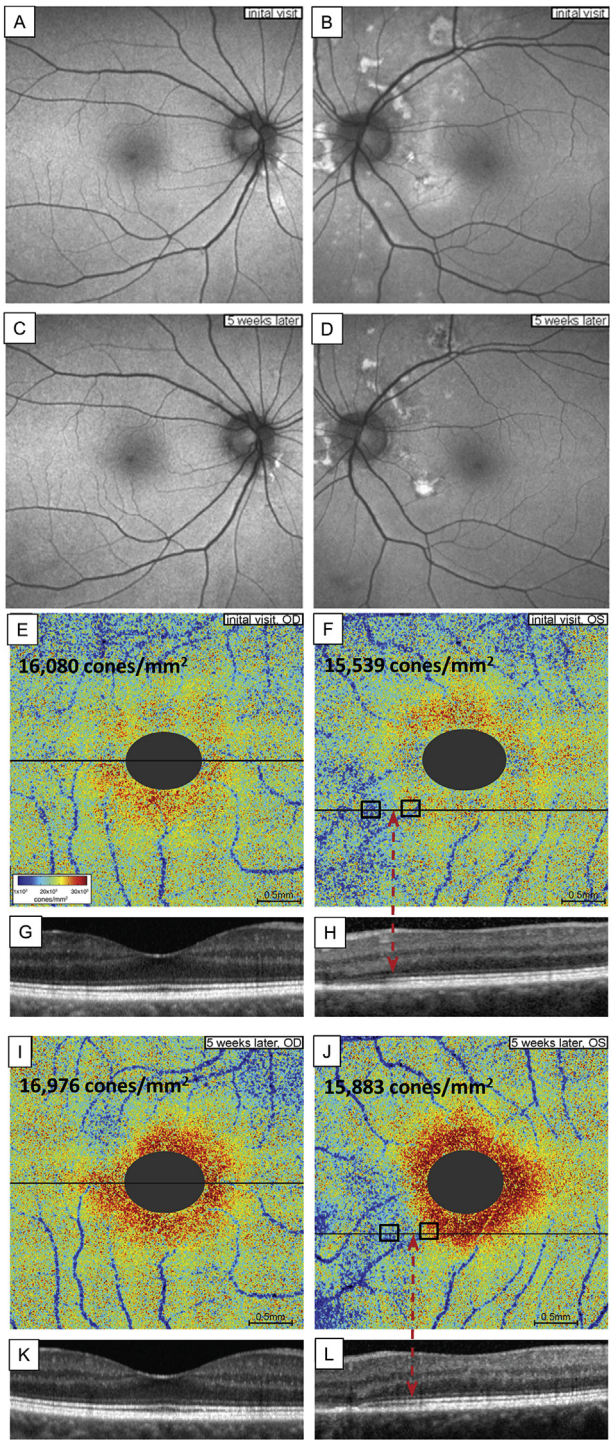

Fig. 2. Improvement in apparent parafoveal cone density after treatment in serpiginous choroidopathy (Case 1). (A–D) Fundus autofluorescence shows lack of parafoveal abnormalities and overall improvement of hyperautofluorescence surrounding lesions after treatment. (E, F) Initial adaptive optics (AO) cone density maps indicating bilateral depression in apparent parafoveal cone density (compared to normal subject in Fig. 1) in absence of optical coherence tomography (OCT) changes in the parafovea (G,H). Areas of ellipsoid zone (EZ) and external limiting membrane (ELM) disruption on OCT (H) are delineated on AO cone density map OS (F), denoted by the red dotted arrow. (I,J) Follow up AO cone density maps after treatment indicating normalization of apparent parafoveal cone density. Areas of EZ and ELM disruption on OCT (L) remain abnormal on AO imaging (J), denoted by the red dotted arrow. The OCT remains normal in the right eye before (G) and after treatment (K) despite improved apparent parafoveal AO cone density (E, I). Black squares in F and J denote 200 μm × 200 μm boxes from which regional cone densities are calculated: the nasal region in F had a cone density of 4451 cones/mm^2 compared to 5170 cones/mm^2 in the same area in J; the parafoveal region in F had a cone density of 15,847 cones/mm^2 and 21,979 cones/mm^2 in J.

presentation) were lower since that area contained a greater proportion of the active area.

2.1.2. Case report 2

A 17 year-old Caucasian emmetropic woman presented with photopsias and small scotomas OD. Her uncorrected visual acuity was 20/20 in both eyes. Fundus examination revealed multifocal small outer retinal lesions in the peripapillary and macular distribution OD, and a normal left eye. FAF showed multifocal hyperautofluorescent lesions (Fig. 3), and FA showed multifocal non-leaking hyperfluorescent lesions in the macula and surrounding the optic nerve, some of which appeared to form a wreath-like configuration suggesting a diagnosis of MEWDS (Fig. S1). SD-OCT, FAF, and AO images in the left eye were normal.

AO images demonstrated distinct multifocal ovoid areas of decreased photoreceptor visualization and decreased apparent cone density in the right macula (Fig. 3A2) while the AO images were normal in the left eye (Fig. S1). These areas were more apparent on the AO cone density map than were indicated by areas of EZ hyporeflectivity on SD-OCT and by hyperautofluorescence on FAF (Fig. 3A). Repeat AO images taken three weeks later, after one week of oral prednisone which was initiated after peripheral and macular progression of the lesions, and then again, after 7 weeks, showed progressive recovery in apparent cone density, which corresponded to normalization in both the FAF and in the photoreceptor inner segment ellipsoid layer on SD-OCT (Fig. 4B–G).

2.1.3. Case report 3

A 34-year old Caucasian woman with moderate myopia (−2.75 OU) presented with decreased vision in the right eye and asymptomatic left eye. The visual acuity was 20/20 in both eyes until she awoke one morning with sudden vision loss to hand motions in the right eye. Examination revealed multifocal outer retinal lesions (Fig. 4A). She had no anterior chamber or vitreous cell in either eye. FAF demonstrated a diffuse area of hyperautofluorescence in the right macula and peripapillary area with satellite lesions of hyperautofluorescence (Fig. 4B). Hypoautofluorescent spots in the temporal and inferotemporal macula corresponded to the retinal lesions seen on examination (Fig. 4B). SD-OCT scans showed macular disruption of the EZ and ELM in the right macula (Fig. 4E). FA, FAF, and SD-OCT (Fig. 4F) imaging were normal in the left eye and her vision remained 20/20 in this eye. The overall findings in this case suggested a most likely diagnosis of multifocal choroiditis with an AZOOR-like acute outer retinal atrophy of the right eye [24,25].

The AO cone density maps demonstrated an apparent diffuse decrease in cone density greatest in the temporal macula (Fig. 4C). Because of the patient's dense central scotoma, the technician noted decreased fixation in the right eye during image acquisition, which led to decreased uniformity in the montage and cone density map in Fig. 4. Surprisingly, AO images in the asymptomatic left eye in which the patient had good fixation with 20/20 visual acuity, revealed an abnormal cone density map showing a diffuse decrease in apparent parafoveal cone density in contrast to her normal fundus appearance, normal SD-OCT, and FAF (Fig. 4F). Initially, full field ERG showed mild cone and rod dysfunction in the right eye and only mildly decreased amplitudes in photopic 30 Hz flicker in the asymptomatic left eye. However, the multifocal ERG showed a marked decrease in amplitudes and prolonged implicit times in the right eye and low-normal responses in the multifocal ERG in the asymptomatic left eye.

After treatment with high dose prednisone, the visual acuity in the right eye improved to 20/400, and there was no change in the AO images of the right eye (not shown). Interestingly, the parafoveal cone mosaic of the left eye also remained unchanged, with persistent areas of decreased cone visualization (Fig. 4G–I). Repeat

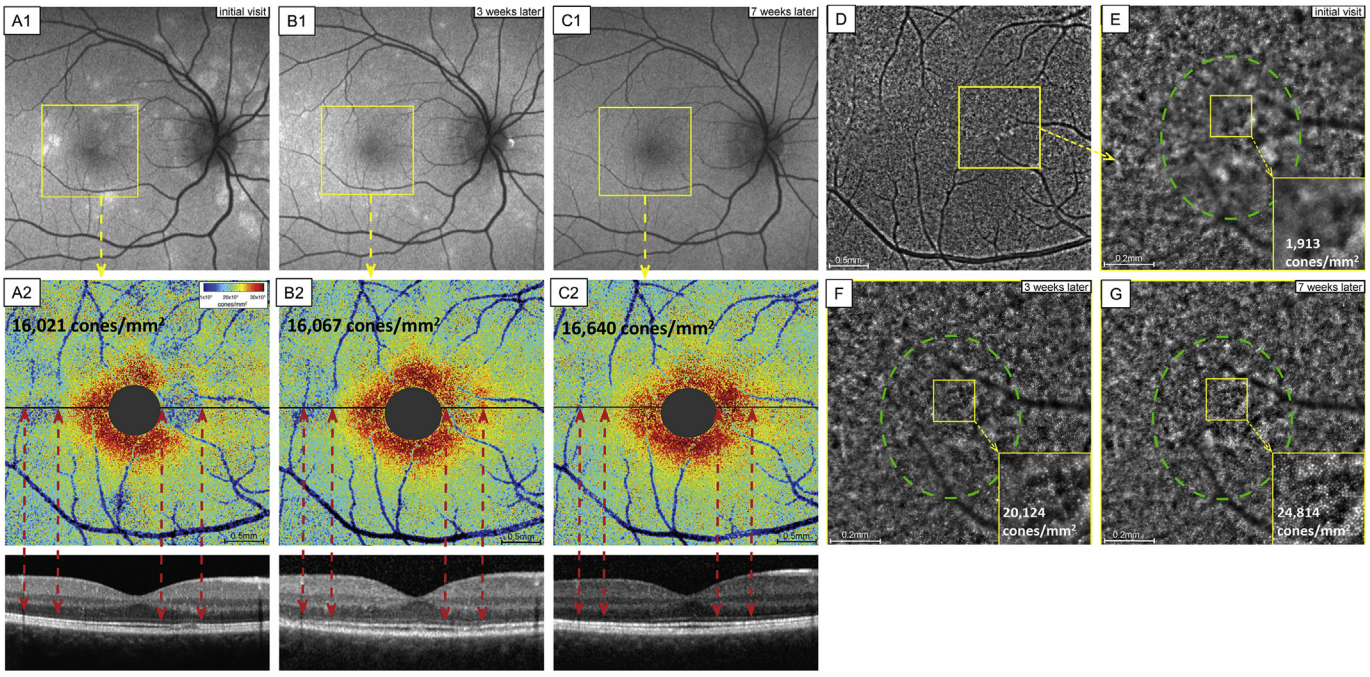

Fig. 3. Improvement in adaptive optics (AO) cone visualization in Multiple Evanescent White Dot Syndrome (MEWDS). (A1-C1) Fundus autofluorescence changes over time. (A2-C2) AO cone density plots from area delineated by yellow square in A1-C1, and corresponding spectral domain-optical coherence tomography (SD-OCT) images demonstrating prominent multifocal areas of ellipsoid disruption and decreased apparent cone density denoted by red dotted arrows initially (column A). 3 weeks later (column B), and 7 weeks later (column C), multi-focal areas of decreased apparent cone density have recovered to normal. (D) 12°×12° AO montage from initial visit and (E) magnified area illustrating oval MEWDS lesion (green dotted oval) containing poorly wave guiding cones (magnified in yellow square insert in lower right), which improved to normal wave guidance in a stepwise fashion (F, G, yellow square inserts in lower right).

full field ERG showed similar findings to the initial test in both eyes, but the multifocal ERG in the asymptomatic left eye was slightly worse compared to the initial test, suggesting that the AO abnormalities may, in some cases, precede consistently altered multifocal ERG responses.

2.1.4. Case report 4

A 29-year old woman who was admitted to the hospital for severe headaches and arthralgias presented with acute vision loss to 20/300 in the right eye and asymptomatic 20/20 left eye. She had extensive ancillary testing and neuroimaging that was unremarkable except for cerebral spinal fluid lymphocytosis. All testing for known infectious or systemic inflammatory conditions was negative. She began treatment with high dose corticosteroids for presumed aseptic meningitis and possible neuroretinitis. While on a prednisone taper from 60 to 50 mg, she developed new visual symptoms with the appearance of multifocal subretinal lesions in the right eye. Her visual acuity at this time had improved to 20/60 in the right eye and remained 20/20 in the left. She reported a persistent central scotoma in the right eye. On examination, multiple outer retinal yellowish lesions were seen in the posterior pole (Fig. 5A) which appeared hyperautofluorescent on FAF (Fig. 5B). An area of mild hypoautofluorescence with a hyperautofluorescent border was noted on FAF (Fig. 5B). SD-OCT showed a distinct area of EZ disruption in the right nasal macula (Fig. 5C1), corresponding to a well-demarcated area highlighted on infrared imaging (Fig. 5E). This patient was also diagnosed with multifocal choroiditis with an AZOOR-like acute outer retinal atrophy [24,25].

AO images taken 9 days after starting high dose prednisone showed a diffuse area of decreased cone visualization (Fig. 5C1–3), and decreased apparent cone density in the nasal macula that corresponded with the appearance seen on infrared photography (Fig. 5E,F) in the right eye. AO images obtained 6 weeks later, after initiating azathioprine and tapering prednisone to 60 mg, illustrated a persistent but stable area of decreased cone visualization on the AO montages in the nasal macula of the right eye (Fig. 5D1–3). AO images of the left eye were normal at initial and follow up visits (Fig. S2).

3. Discussion

The AO flood illumination camera revealed decreased cone visualization and decreased apparent cone densities in four cases of posterior uveitis. Our software identifies cones through a maximum threshold level of reflectivity. A decrease in the cone density map could therefore correspond to a disappearance of cones or a decrease in cone reflectivity due to a variety of causes [26]. In our study, these AO patterns corresponded to visual symptoms in some patients, but not in others. We postulate that AO cone reflectivity may be a measure of disruption of the outer segment structure rather than cell death since there was recovery of non-wave guiding to wave guiding cones in some cases. More studies looking at cone reflective properties are warranted for better localization and a clearer understanding of the underlying etiology of observed abnormalities on AO imaging.

Case report 1 provides unique findings in serpiginous choroiditis. Acute lesions are thought to occur predominantly in the RPE and choroicapillaris in serpiginous choroiditis with progressive atrophy extending into the outer retina as the acute lesions clear [27]. AO images in our case correspond to this clinical pattern with persistent areas of decreased cone visualization in areas of persistent ELM and EZ disruption on SD-OCT. Another novel finding was the loss of apparent parafoveal cone density in both eyes despite 20/20 vision, which recovered to normal after treatment. SD-OCT appeared normal in these areas suggesting that AO may not always correlate with SD-OCT findings.

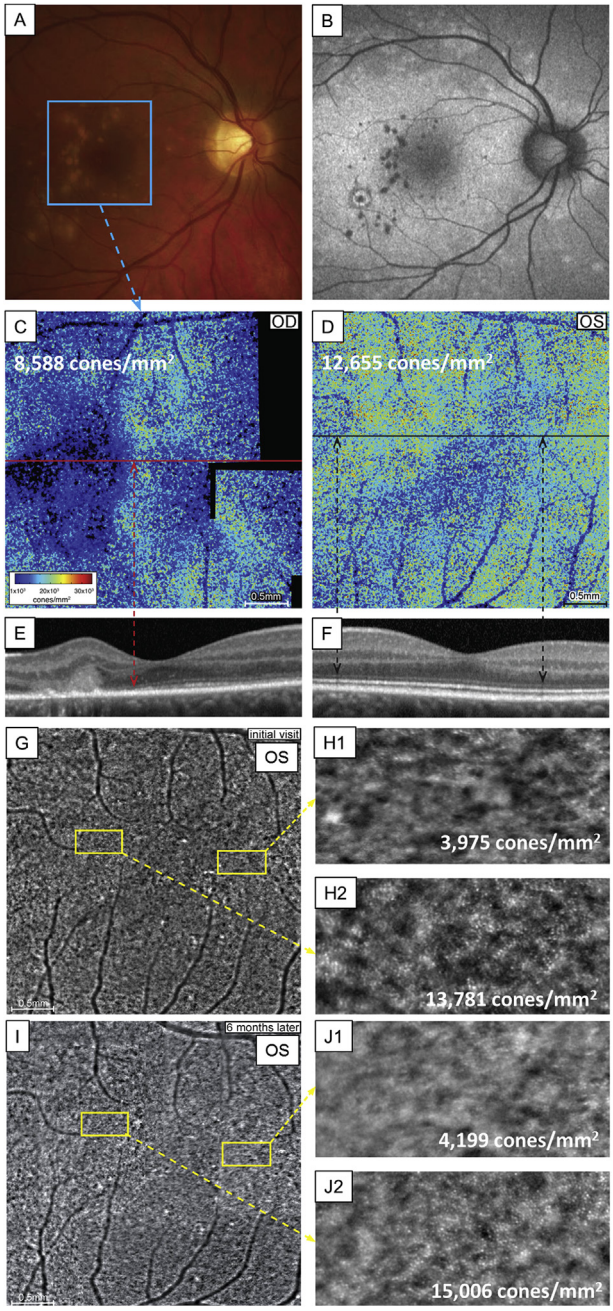

Fig. 4. Decreased adaptive optics (AO) apparent cone density in multifocal choroiditis with acute outer retinal atrophy (Case 3) persists with treatment. (A) Fundus image and (B) fundus autofluorescence of symptomatic right eye. (C,D) AO cone density maps of right and left eyes, demonstrating expected diffuse apparent decreased cone density OD (C), and unexpected decreased cone density OS (D). (E) Corresponding ellipsoid zone and external limiting membrane disruptions on spectral domain-optical coherence tomography (SD-OCT) denoted by red arrow and relatively normal SD-OCT OS (F). (G–H) AO montage of asymptomatic left eye at initial visit as well as selected highly magnified areas of decreased cone visualization (H1, H2). (I–J) AO montage of asymptomatic left eye at 6 month follow up visit after initiation of treatment demonstrating persistent areas of decreased cone visualization, magnified in J1-J2.

Case report 2 is unique in its documentation of the recovery of photoreceptor abnormalities by AO in MEWDS. AO recovery corresponded to resolution of subjective scotomas, suggesting a correlation between the altered reflectance patterns and visual function in this case. The outer retina and RPE layers have been the postulated sites of pathology in MEWDS based on previous reports using SD-OCT and FAF [5,6,9,28]. The abnormal AO images seen in our case supports the notion of photoreceptor outer segment involvement as the predominant site of disease in MEWDS, as changes were most apparent on AO images. Our findings correspond to the previous case reports of AO in MEWDS, which also reported altered photoreceptor imaging [2,22].

Case reports 3 and 4 had vision loss out of proportion to exam findings. AO in conjunction with SD-OCT highlighted photoreceptor disruption that accounted for the severe central vision loss. Abnormal AO findings in the symptomatic eye in Case 3 was associated with an abnormal full field ERG, supporting the theory that AO abnormalities may correlate with decreased photoreceptor function. Case report 3 also showed a decrease in apparent cone density in the contralateral asymptomatic eye despite no identifiable risk factors for decreased image quality in this eye. Although unknown risk factors affecting image quality may exist, the worsening multifocal ERG and persistent AO abnormalities upon repeat testing in the asymptomatic left eye supports the notion that the AO findings were true abnormalities, and may in this case be more sensitive than multifocal ERG testing in detecting subclinical change.

As this series included a small number of heterogeneous posterior uveitides, limitations exist in estimating the reliability and reproducibility of AO patterns seen within each case and clinical entity. A potential learning curve in patient fixation may affect image quality and cone density measurements at subsequent imaging sessions. Repeatability measurements among a normative database collected under the same study protocol had an average coefficient of variation in cone densities of less than 2% between AO imaging sessions [23]. The improvement in apparent parafoveal cone density in Case 1 and 2 after treatment appear to be much higher than this average variability, suggesting true recovery, rather than improvements from learning. Cases 3 and 4 also suggest reliable findings since there were reproducible areas of disrupted photoreceptor visualization upon subsequent AO imaging.

A prospective series by Agarwal and colleagues in posterior uveitides also used AO flood illumination imaging to demonstrate decreased cone densities in active lesions [21]. In their study, there appeared to be an association between cone density and the active or inactive state, although the difference was not statistically significant, likely due to the heterogeneity of diseases included. Our study also included 4 heterogeneous types of posterior uveitis, and the individual cases presented here highlight how 4 different conditions can have very disparate AO abnormalities at initial presentation and throughout the course of the disease.

4. Conclusions

This study demonstrates that a flood illuminated AO camera is able to delineate subclinical photoreceptor abnormalities in posterior uveitis affecting the outer retina. As additional patients with these entities are imaged longitudinally, adaptive optics may prove to be useful in providing a better understanding of disease progression, in identifying possible prognostic factors, and in following response to treatment.

Competing interests

A travel grant was provided by Imagine Eyes to MEP. The authors indicate no other competing interests.

Funding

PL and MEP are supported by Research to Prevent Blindness (RPB) Career Development Awards; PL by NEI K08EY022948 and a Collins Medical Trust foundation award; MEP by Foundation

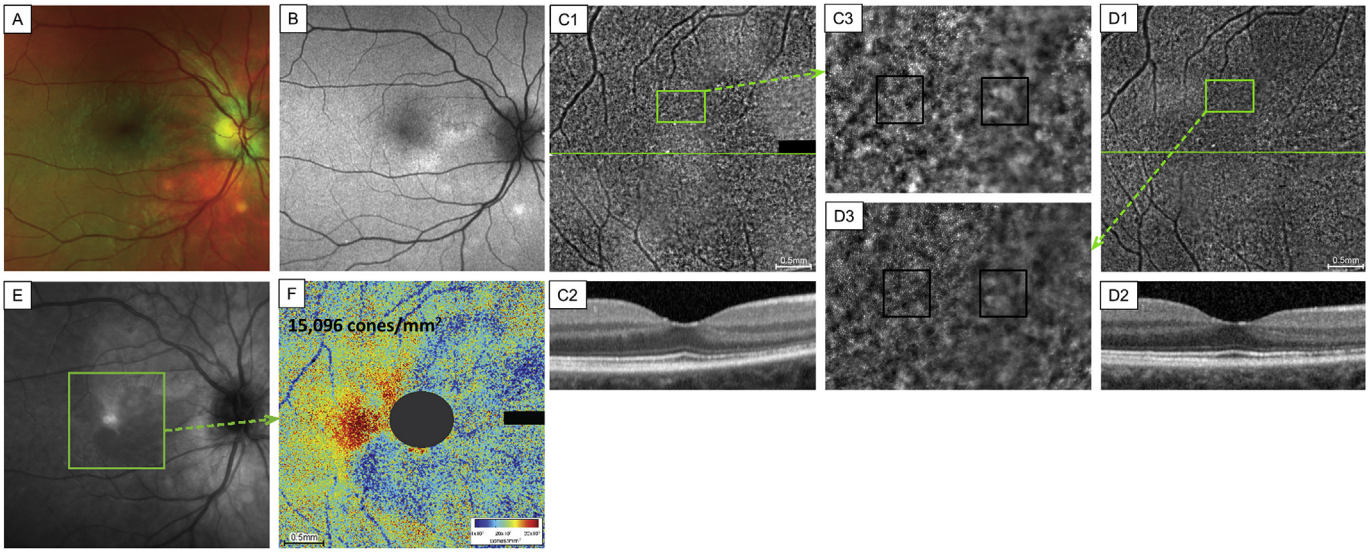

Fig. 5. Decreased adaptive optics (AO) apparent cone density in second patient who had multifocal choroiditis with acute outer retinal atrophy (Case 4) persists with treatment. (A) Fundus image and (B) fundus autofluorescence of symptomatic right eye. Early treatment AO montage (C1), magnified montage (C3), and spectral domain-optical coherence tomography (SD-OCT) images (C2), compared to follow-up images 6 weeks after initiation of treatment (D1-D3) reveals persistently decreased AO cone visualization and ellipsoid zone disruption on OCT. Black squares in C3 and D3 denote a 200 μm × 200 μm box from which cone density was sampled regionally. Values are the following: C3-left, 15,799; C3-right, 112; D3-left, 18,713; D3-right, 82 cones/mm^2; (E) Infrared image and (F) AO cone density map, demonstrating corresponding well-delineated area of decreased apparent cone density.

Fighting Blindness Career Development Award (CD-CL-0808-0469-OHSU), NEI award K08EY0201186, and an ARVO/Alcon Young Clinician Scientist Research Award; MJG by a Fight For Sight Summer Student Fellowship (FFS-SS-12-010); TBS is supported by a Fight for Sight Grant-in Aid Award (FFS-GIA-13-020). This research was also partially supported by departmental core grant P30 EY010572 and a departmental unrestricted RPB grant.

Acknowledgments

None.

Appendix A. Supplementary data

Supplementary data related to this article can be found at http://dx.doi.org/10.1016/j.ajoc.2016.03.001.

References

[1] T.E. Arantes, K. Matos, C.R. Garcia, T.G. Silva, A.S. Sabrosa, C. Muccioli, Fundus autofluorescence and spectral domain optical coherence tomography in recurrent serpiginous choroiditis: case report, Ocul. Immunol. Inflamm. 19 (1) (2011) 39–41, http://dx.doi.org/10.3109/09273948.2010.515373 (published Online First: Epub Date).

[2] A. Boretsky, S. Mirza, F. Khan, M. Motamedi, F.J. van Kuijk, High-resolution multimodal imaging of multiple evanescent white dot syndrome, Ophthalmic Surg. Lasers Imaging Retina 44 (3) (2013) 296–300, http://dx.doi.org/10.3928/23258160-20130503-18 (published Online First: Epub Date)|.

[3] F. Cardillo Piccolino, A. Grosso, E. Savini, Fundus autofluorescence in serpiginous choroiditis, Graefe's Arch. Clin. Exp. Ophthalmol. = Albrecht von Graefes Archiv fur klinische und experimentelle Ophthalmologie 247 (2) (2009) 179–185, http://dx.doi.org/10.1007/s00417-008-0951-z (published Online First: Epub Date)|.

[4] F.T. da Silva, V.M. Sakata, A. Nakashima, et al., Enhanced depth imaging optical coherence tomography in long-standing Vogt-Koyanagi-Harada disease, Br. J. Ophthalmol. 97 (1) (2013) 70–74, http://dx.doi.org/10.1136/bjophthalmol-2012-302089 (published Online First: Epub Date)|.

[5] C. Furino, F. Boscia, N. Cardascia, G. Alessio, C. Sborgia, Fundus autofluorescence and multiple evanescent white dot syndrome, Retina 29 (1) (2009) 60–63, http://dx.doi.org/10.1097/IAE.0b013e31818c5e04 (published Online First: Epub Date)|.

[6] D. Li, S. Kishi, Restored photoreceptor outer segment damage in multiple evanescent white dot syndrome, Ophthalmology 116 (4) (2009) 762–770, http://dx.doi.org/10.1016/j.ophtha.2008.12.060 (published Online First: Epub Date)|.

[7] P. Lin, P.S. Mettu, D.L. Pomerleau, et al., Image inversion spectral-domain optical coherence tomography optimizes choroidal thickness and detail through improved contrast, Investig. Ophthalmol. Vis. Sci. 53 (4) (2012) 1874–1882, http://dx.doi.org/10.1167/iovs.11-9290 (published Online First: Epub Date)|.

[8] M. Nakayama, H. Keino, A.A. Okada, et al., Enhanced depth imaging optical coherence tomography of the choroid in Vogt-Koyanagi-Harada disease, Retina 32 (10) (2012) 2061–2069, http://dx.doi.org/10.1097/IAE.0b013e318256205a (published Online First: Epub Date)|.

[9] B.J. Thomas, T.A. Albini, H.W. Flynn Jr., Multiple evanescent white dot syndrome: multimodal imaging and correlation with proposed pathophysiology, Ophthalmic Surg. Lasers Imaging Retina 44 (6) (2013) 584–587, http://dx.doi.org/10.3928/23258160-20131015-03 (published Online First: Epub Date)|.

[10] S. Yeh, F. Forooghian, W.T. Wong, et al., Fundus autofluorescence imaging of the white dot syndromes, Arch. Ophthalmol. 128 (1) (2010) 46–56, http://dx.doi.org/10.1001/archophthalmol.2009.368 (published Online First: Epub Date)|.

[11] R.C. Baraas, J. Carroll, K.L. Gunther, et al., Adaptive optics retinal imaging reveals S-cone dystrophy in tritan color-vision deficiency, J. Opt. Soc. Am. A Opt. Image Sci. Vis. 24 (5) (2007) 1438–1447.

[12] J. Carroll, M. Neitz, H. Hofer, J. Neitz, D.R. Williams, Functional photoreceptor loss revealed with adaptive optics: an alternate cause of color blindness, Proc. Natl. Acad. Sci. U. S. A. 101 (22) (2004) 8461–8466, http://dx.doi.org/10.1073/pnas.0401440101 (published Online First: Epub Date)|.

[13] E.W. Dees, A. Dubra, R.C. Baraas, Variability in parafoveal cone mosaic in normal trichromatic individuals, Biomed. Opt. Express 2 (5) (2011) 1351–1358, http://dx.doi.org/10.1364/BOE.2.001351 (published Online First: Epub Date)|.

[14] J.L. Duncan, Y. Zhang, J. Gandhi, et al., High-resolution imaging with adaptive optics in patients with inherited retinal degeneration, Investig. Ophthalmol. Vis. Sci. 48 (7) (2007) 3283–3291, http://dx.doi.org/10.1167/iovs.06-1422 (published Online First: Epub Date)|.

[15] H. Hofer, B. Singer, D.R. Williams, Different sensations from cones with the same photopigment, J. Vis. 5 (5) (2005) 444–454, http://dx.doi.org/10.1167/5.5.5 (published Online First: Epub Date)|.

[16] A. Roorda, D.R. Williams, The arrangement of the three cone classes in the living human eye, Nature 397 (6719) (1999) 520–522, http://dx.doi.org/10.1038/17383 (published Online First: Epub Date)|.

[17] J.I. Wolfing, M. Chung, J. Carroll, A. Roorda, D.R. Williams, High-resolution retinal imaging of cone-rod dystrophy, Ophthalmology 113 (6) (2006) 1019 e1, http://dx.doi.org/10.1016/j.ophtha.2006.01.056 (published Online First: Epub Date)|.

[18] S.O. Hansen, R.F. Cooper, A. Dubra, J. Carroll, D.V. Weinberg, Selective cone photoreceptor injury in acute macular neuroretinopathy, Retina 33 (8) (2013) 1650–1658, http://dx.doi.org/10.1097/IAE.0b013e31828cd03a (published Online First: Epub Date)|.

[19] M. Mkrtchyan, B.J. Lujan, D. Merino, C.E. Thirkill, A. Roorda, J.L. Duncan, Outer retinal structure in patients with acute zonal occult outer retinopathy, Am. J. Ophthalmol. 153 (4) (2012) 757–768, 68 e1 doi: 10.1016/j.ajo.2011.09.007(-published Online First: Epub Date)|.

[20] S. Mrejen, R. Gallego-Pinazo, K.J. Wald, K.B. Freund, Acute posterior multifocal placoid pigment epitheliopathy as a choroidopathy: what we learned from adaptive optics imaging, JAMA Ophthalmol. 131 (10) (2013) 1363–1364, http://dx.doi.org/10.1001/jamaophthalmol.2013.4196 (published Online First: Epub Date)|.

[21] A. Agarwal, M.K. Soliman, M. Hanout, et al., Adaptive optics imaging of retinal photoreceptors overlying lesions in white dot syndrome and its functional correlation, Am. J. Ophthalmol. 160 (4) (2015) 806–816 e2 doi: 10.1016/j.ajo.2015.07.013(published Online First: Epub Date)|.

[22] L.T. Labriola, A.D. Legarreta, J.E. Legarreta, et al., Imaging with multimodal adaptive-optics optical coherence tomography in multiple evanescent white dot syndrome: the structure and functional relationship, Retin. Cases Brief Rep. (2016), http://dx.doi.org/10.1097/ICB.0000000000000271 (published Online First: Epub Date)|.

[23] S. Feng, M.J. Gale, J.D. Fay, et al., Assessment of different sampling methods for measuring and representing macular cone density using flood-illuminated adaptive optics, Investig. Ophthalmol. Vis. Sci. 56 (10) (2015) 5751–5763, http://dx.doi.org/10.1167/iovs.15-16954 (published Online First: Epub Date)|.

[24] J.J. Jung, S. Khan, S. Mrejen, et al., Idiopathic multifocal choroiditis with outer retinal or chorioretinal atrophy, Retina 34 (7) (2014) 1439–1450, http://dx.doi.org/10.1097/IAE.0000000000000079 (published Online First: Epub Date)|.

[25] M.R. Munk, J.J. Jung, K. Biggee, et al., Idiopathic multifocal choroiditis/punctate inner choroidopathy with acute photoreceptor loss or dysfunction out of proportion to clinically visible lesions, Retina 35 (2) (2015) 334–343, http://dx.doi.org/10.1097/IAE.0000000000000370 (published Online First: Epub Date)|.

[26] W. Makous, J. Carroll, J.I. Wolfing, J. Lin, N. Christie, D.R. Williams, Retinal microscotomas revealed with adaptive-optics microflashes, Investig. Ophthalmol. Vis. Sci. 47 (9) (2006) 4160–4167, http://dx.doi.org/10.1167/iovs.05-1195 (published Online First: Epub Date)|.

[27] I.H. Chisholm, J.D. Gass, W.L. Hutton, The late stage of serpiginous (geographic) choroiditis, Am. J. Ophthalmol. 82 (3) (1976) 343–351.

[28] L.M. Jampol, P.A. Sieving, D. Pugh, G.A. Fishman, H. Gilbert, Multiple evanescent white dot syndrome. I. Clinical findings, Arch. Ophthalmol. 102 (5) (1984) 671–674.